

AD-A230 110

FILE COPY

Subthreshold I-V Characteristics of AlGaAs/GaAs MODFETs: The Role of Unintentional Acceptors

Prepared by

R. J. KRANTZ and W. L. BLOSS
Electronics Research Laboratory
Laboratory Operations

19 October 1990

Prepared for

SPACE SYSTEMS DIVISION
AIR FORCE SYSTEMS COMMAND
Los Angeles Air Force Base
P.O. Box 92960
Los Angeles, CA 90009-2960

Development Group

THE AEROSPACE CORPORATION
El Segundo, California

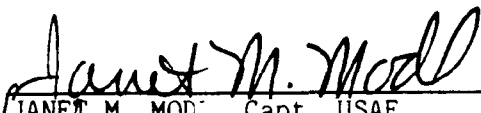
APPROVED FOR PUBLIC RELEASE;
DISTRIBUTION UNLIMITED


DTIC
ELECTE
DEC 17 1990
S D

This report was submitted by The Aerospace Corporation, El Segundo, CA 90245, under Contract No. F04701-88-C-0089 with the Space Systems Division, P.O. Box 92960, Los Angeles, CA 90009-2960. It was reviewed and approved for The Aerospace Corporation by M. J. Daugherty, Director, Electronics Research Laboratory. Captain Janet Modl was the Air Force project officer for the Mission-Oriented Investigation and Experimentation (MOIE) program.

This report has been reviewed by the Public Affairs Office (PAS) and is releasable to the National Technical Information Service (NTIS). At NTIS, it will be available to the general public, including foreign nationals.

This technical report has been reviewed and is approved for publication. Publication of this report does not constitute Air Force approval of the report's findings or conclusions. It is published only for the exchange and stimulation of ideas.


JANET M. MODL, Capt, USAF
MOIE Project Officer
STC/SWL


JONATHAN M. EMMES, Maj, USAF
MOIE Program Manager
AFSTC/WCO OL-AB

UNCLASSIFIED

SECURITY CLASSIFICATION OF THIS PAGE

REPORT DOCUMENTATION PAGE

1a REPORT SECURITY CLASSIFICATION Unclassified			1b RESTRICTIVE MARKINGS		
2a SECURITY CLASSIFICATION AUTHORITY			3 DISTRIBUTION/AVAILABILITY OF REPORT Approved for public release; distribution unlimited.		
2b DECLASSIFICATION/DOWNGRADING SCHEDULE					
4. PERFORMING ORGANIZATION REPORT NUMBER(S) TR-0090(5925-01)-2			5. MONITORING ORGANIZATION REPORT NUMBER(S) SSD-TR-90-46		
6a NAME OF PERFORMING ORGANIZATION The Aerospace Corporation Laboratory Operations		6b OFFICE SYMBOL (If applicable)		7a NAME OF MONITORING ORGANIZATION Space Systems Division	
6c ADDRESS (City, State, and ZIP Code) El Segundo, CA 90245-4691			7b ADDRESS (City, State, and ZIP Code) Los Angeles Air Force Base Los Angeles, CA 90009-2960		
8a NAME OF FUNDING/SPONSORING ORGANIZATION		8b OFFICE SYMBOL (If applicable)		9 PROCUREMENT INSTRUMENT IDENTIFICATION NUMBER F04701-88-C-0089	
8c ADDRESS (City, State, and ZIP Code)			10. SOURCE OF FUNDING NUMBERS		
			PROGRAM ELEMENT NO.	PROJECT NO.	TASK NO.
			WORK UNIT ACCESSION NO.		
11. TITLE (Include Security Classification) Subthreshold I-V Characteristics of AlGaAs/GaAs MODFETs: The Role of Unintentional Acceptors					
12 PERSONAL AUTHOR(S) Krantz, Richard J. and Bloss, Walter L.					
13a TYPE OF REPORT		13b TIME COVERED FROM _____ TO _____		14 DATE OF REPORT (Year, Month, Day) 1990 October 19	
				15 PAGE COUNT 16	
16 SUPPLEMENTARY NOTATION					
17 COSATI CODES			18 SUBJECT TERMS (Continue on reverse if necessary and identify by block number)		
FIELD	GROUP	SUB-GROUP			
			MODFETs		
			Subthreshold		
19 ABSTRACT (Continue on reverse if necessary and identify by block number)					
<p>A strong inversion, depletion layer model of threshold has been extended to describe subthreshold I-V characteristics in MODFETs (modulation doped field-effect transistors). The results of this calculation yield the MODFET equivalent of the MOSFET (metal-oxide semiconductor field-effect transistor) charge sheet subthreshold model. For typical molecular beam epitaxy (MBE) grown structure, the subthreshold current may differ by two-orders of magnitude for a given gate voltage V_g and drain-to-source voltage V_{ds} as the acceptor doping varies from 10^{13} to 10^{15} cm^{-3}. For these acceptor doping densities, the gate voltage, for a given drain-to-source voltage, needed to maintain a constant subthreshold current, varies by only $\sim 0.1 \text{ V}$. If the acceptor density is increased to 10^{17} cm^{-3}, a large increase ($\sim 0.8 \text{ V}$) in the gate voltage is required to maintain a constant subthreshold current. These changes in subthreshold current with acceptor concentration in the bulk GaAs are significant and need to be included in an accurate MODFET model.</p>					
20 DISTRIBUTION/AVAILABILITY OF ABSTRACT <input checked="" type="checkbox"/> UNCLASSIFIED/UNLIMITED <input type="checkbox"/> SAME AS RPT <input type="checkbox"/> DTIC USERS			21. ABSTRACT SECURITY CLASSIFICATION Unclassified		
22a NAME OF RESPONSIBLE INDIVIDUAL			22b. TELEPHONE (Include Area Code)		22c OFFICE SYMBOL

CONTENTS

I.	INTRODUCTION.....	5
II.	MATHEMATICAL PROPERTIES NEAR THRESHOLD.....	9
III.	SUBTHRESHOLD I-V CHARACTERISTICS.....	11
IV.	SUMMARY.....	15
	REFERENCES.....	17



Accession For	
NTIS CRA&I	<input checked="" type="checkbox"/>
DTIC TAB	<input type="checkbox"/>
Unannounced	<input type="checkbox"/>
Justification	
By	
Distribution /	
Availability Codes	
Dist	Avail and/or Special
A-1	

FIGURES

1.	Band Diagram of a Typical AlGaAs/GaAs MODFET with Schottky Gate, under Bias V_g	7
2.	Function $f(n_s)$ versus Channel Carrier Density Density for Two Extremes of Acceptor Density.....	10
3.	MODFET Subthreshold Current versus Applied Gate Voltage.....	13

I. INTRODUCTION

The dependence of the threshold voltage and radiation response of n-channel AlGaAs/GaAs MODFETs (modulation doped field-effect transistors) on acceptor doping density has been described previously (Refs. 1-3). These analyses have now been extended to describe the dependence of MODFET subthreshold I-V characteristics on acceptor doping density.

The band structure of a typical AlGaAs(n)/GaAs heterojunction with Schottky barrier, ϕ_m , at the gate, and a spacer layer at the interface under bias V_g , is shown in Fig. 1. In the depletion layer approximation, the donors and acceptors are assumed to be completely ionized in the doped AlGaAs layer d , the spacer layer a , and in the depletion layer W . The doping densities N_D and N_A are assumed constant. The quasi-two-dimensional electron eigenstates at the interface are solved for using a triangular potential well, and only the lowest subband is included in the calculation. A delta-function channel charge distribution at the average channel width is assumed. Band bending from the interface at $(d + a)$ to the edge of the depletion region $(W + d + a)$ is the difference of the position of the conduction band relative to the Fermi level in the GaAs far from the interface ($E_g/2 + \phi_{\text{bulk}}$) and the Fermi level E_f relative to the bottom of the two-dimensional channel.

Under the restrictions imposed by these assumptions, Poisson's equation may be integrated across the structure to obtain the applied gate voltage as a function of device geometry, doping densities, and channel charge n_s :

$$V_g = V_0 + f(n_s) \quad (1)$$

where V_0 is the difference between the Schottky barrier height and the sum of the band offset and potential drop across the doped AlGaAs layer due to the ionized donors. The function $f(n_s)$ may be written as:

$$f(n_s) = (q/\epsilon)(d + a)(N_A W + n_s) + C_0(N_A W + n_s)^{2/3} + (kT/q)\ln[\exp(n_s/n_c) - 1] \quad (2)$$

where C_0 is a function of the Planck constant, the carrier effective mass, the elemental charge, and the permittivity of AlGaAs and GaAs, assumed identical. C_0 is equal to $-1.7 \times 10^{-9} \text{ V-cm}^{4/3}$. Similarly, the charge density n_c is a function of physical constants and the effective carrier mass and is equal to $-8.4 \times 10^{11} \text{ cm}^{-2}$. The quantities q , ϵ , k , and T are elemental charge, AlGaAs(GaAs) permittivity (assumed identical), Boltzmann constant, and absolute temperature. A discussion of the dependence of the depletion width W on acceptor density has been given elsewhere (Ref. 1). In section II we describe the mathematical properties of the function $f(n_s)$, near threshold. In section II we exploit these properties to derive the subthreshold characteristics of these devices.

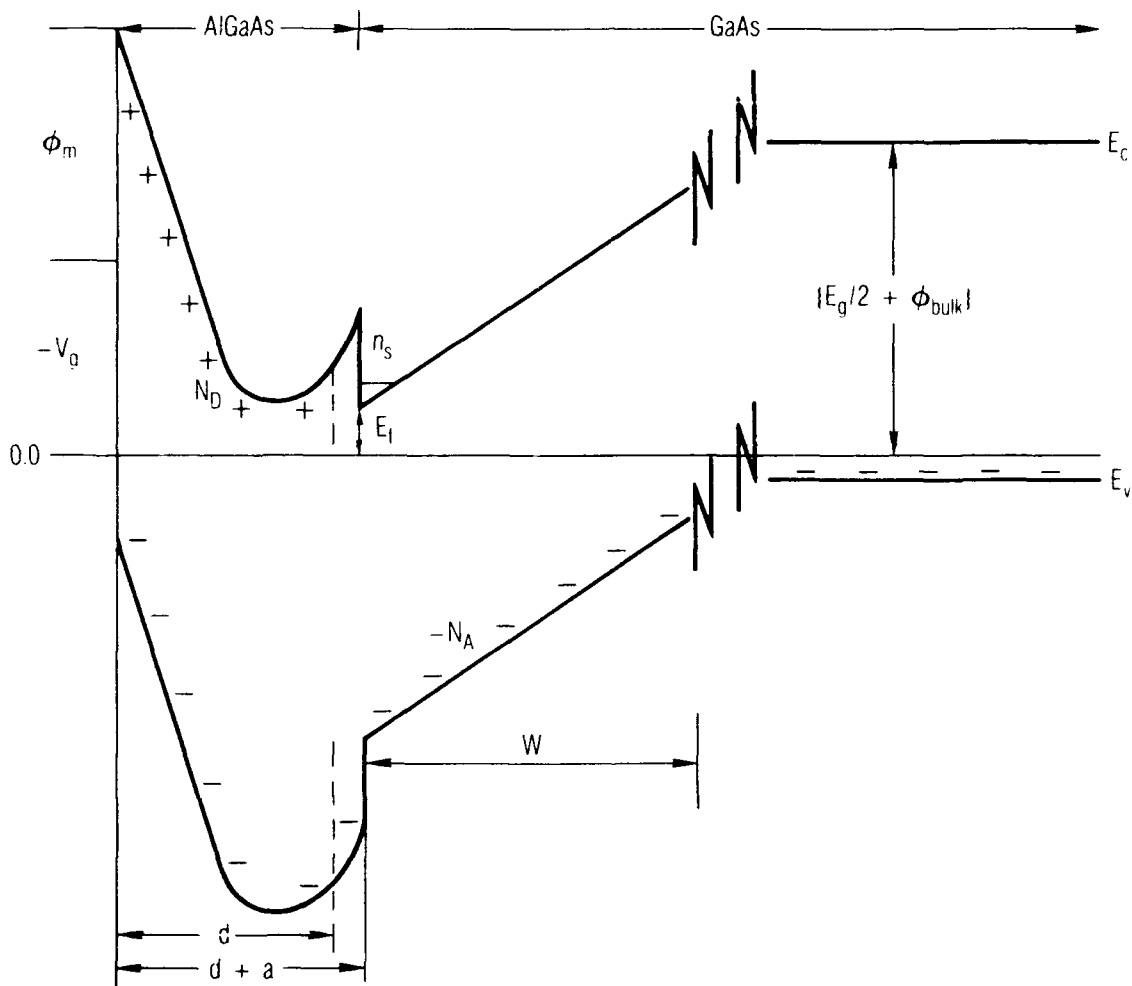


Fig. 1. Band Diagram of a Typical AlGaAs/GaAs MODFET with Schottky Gate, under bias V_g .

II. MATHEMATICAL PROPERTIES NEAR THRESHOLD

At threshold, the channel density may be defined as equal to the acceptor density N_A times the average channel width z_{av} , which may be calculated in the triangular-well approximation using variational wave functions (Refs. 4, 5). This definition of threshold is equivalent to that used for MOSFETs (metal-oxide semiconductor field-effect transistors). Calculation of the threshold carrier density is described elsewhere (Ref. 1). In the subthreshold region, where $n_S \sim N_A z_{av} \ll N_A W$, Eq. (2) may be approximated as

$$f(n_S) = (q/\epsilon)(d + a)N_A + C_0(N_A W)^{2/3} + (kT/q)\ln(n_S/n_c) \quad (3)$$

In Fig. 2, $f(n_S)$ versus n_S is shown for two extremes of the acceptor density. The solid curves are the results of Eq. (2), and the dashed curves are the results of Eq. (3).

The approximation is almost identical to the exact results to channel densities up to 10^{10} cm^{-2} . The approximate results do not diverge significantly from the exact results until the channel density is above 10^{11} cm^{-2} . Letting

$$V_0' = V_0 + (q/\epsilon)(d + a)N_A W + C_0(N_A W)^{2/3} \quad (4)$$

the applied gate voltage in the subthreshold region, $V_{g\text{sub}}$, is related to the channel charge in the following way:

$$V_{g\text{sub}} = V_0' + (kT/q)\ln(n_S/n_c). \quad (5)$$

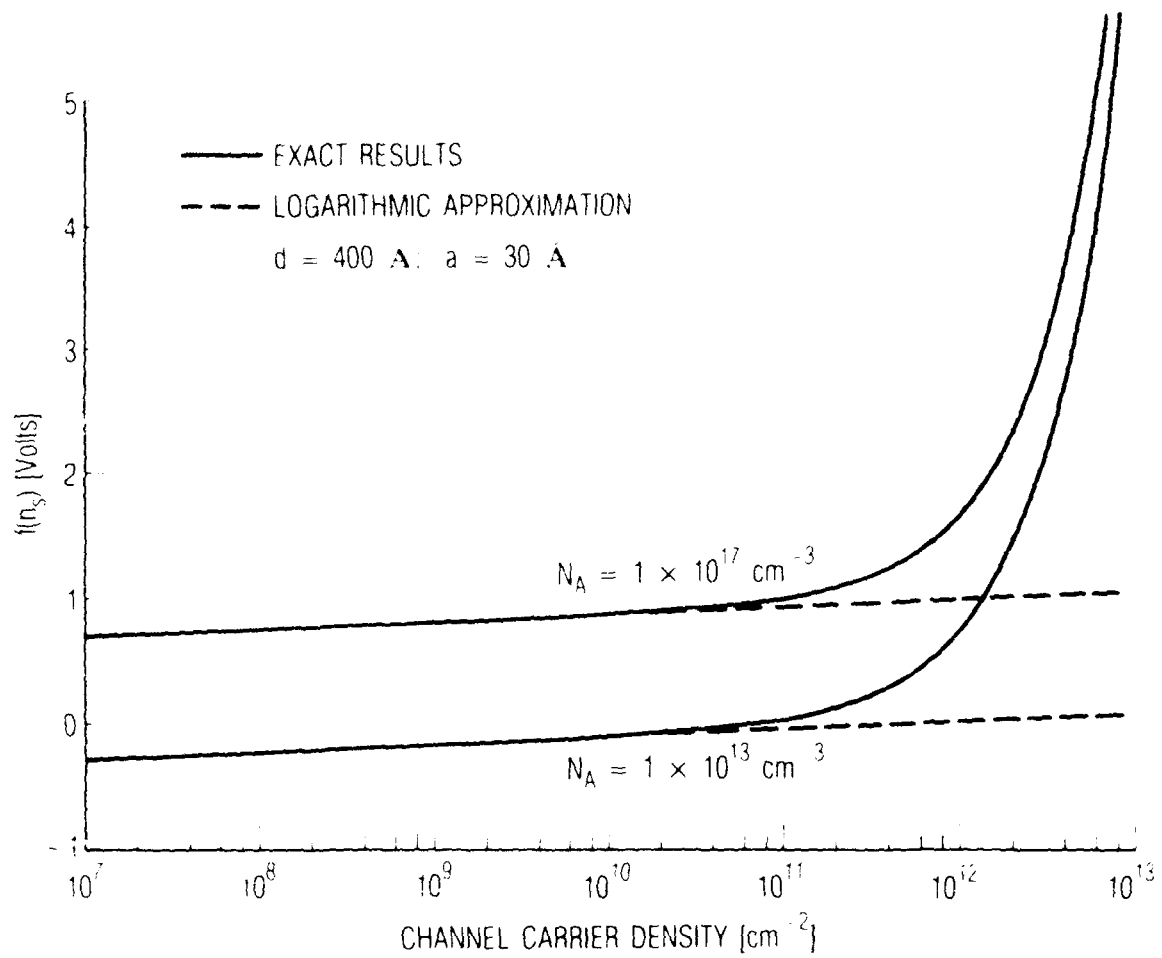


Fig. 2. Function $f(n_s)$ versus Channel Carrier Density for Two Extremes of Acceptor Density. The solid curves are the exact results of Eq. (2); the dashed lines are the results of the logarithmic approximation, described in text.

III. SUBTHRESHOLD I-V CHARACTERISTICS

In the gradual channel approximation, charge control is determined by the effective potential in the channel:

$$V(x) = V_{gsub} - V_c(x) \quad (6)$$

where $V_c(x)$ is the channel voltage under the gate at point x . Using Eqs. (5) and (6) we solve for the carrier density in the channel:

$$n_s(x) = n_c \exp\left\{\frac{q}{kT}[V_{gsub} - V_0' - V_c(x)]\right\} \quad (7)$$

The form of Eq. (7) allows the source-drain current to be calculated in the usual way (Ref. 6). The result is

$$I_{sub} = kTu(Z/L)n(0)\{1 - \exp[-q(V_D - V_S)/kT]\} \quad (8)$$

where

$$n(0) = n_c \exp[q(V_{gsub} - V_0' - V_S)/kT] \quad (9)$$

u = channel mobility

Z = channel width

L = channel length

Equation (8) is the MODFET equivalent of the charge sheet subthreshold current derived by Brews (Ref. 7). In the subthreshold region (i.e., the channel charge in the whole channel is of the order of the threshold carrier density), the source-to-drain voltage is small, and the exponentials containing these terms may be linearized.

The subthreshold current versus the applied gate voltage for various acceptor doping densities is shown in Fig. 3 for the device parameters listed. Source and drain resistances have been ignored. The dashed line is the current produced for a constant channel carrier density of 10^{11} cm^{-2} throughout the channel. Our subthreshold approximation of $f(n_g)$ diverges from Eq. (2) in this range. Therefore, the subthreshold current calculation is unreliable for this range of carrier densities. Device source-drain currents will depart from the subthreshold currents shown at about 0.1 nA for the device parameters shown. The observed subthreshold current at very large acceptor doping may include a contribution from conduction through the undepleted region of the bulk p-GaAs. This effect has been ignored in our calculation.

At low subthreshold currents, 0.1 - 1 nA, the subthreshold currents are constant with decreasing gate bias. In this region a large change in $V_{g\text{sub}}$ is required to produce a relatively small change in the channel carrier density.

The dependence of the subthreshold current on acceptor density is clearly demonstrated. Even for the relatively low unintentional acceptor doping densities that result from typical molecular beam epitaxy (MBE) growth, $10^{13} - 10^{15} \text{ cm}^{-3}$, the subthreshold current will vary by two orders of magnitude over this range for a given applied gate voltage. For acceptor doping densities well above this range, the subthreshold I-V characteristics will shift some 0.8 to 0.9 V as shown.

The subthreshold conductance, in the limit of small drain-source voltage and zero drain-source resistance, is given by the subthreshold current divided by the drain-source voltage and, therefore, has the same dependence on V_{DS} and V_g as the subthreshold current, as shown in Fig. 3. The subthreshold transconductance, under the same limitations, is given by the subthreshold current divided by kT/q , which also has the same functional form as the subthreshold current.

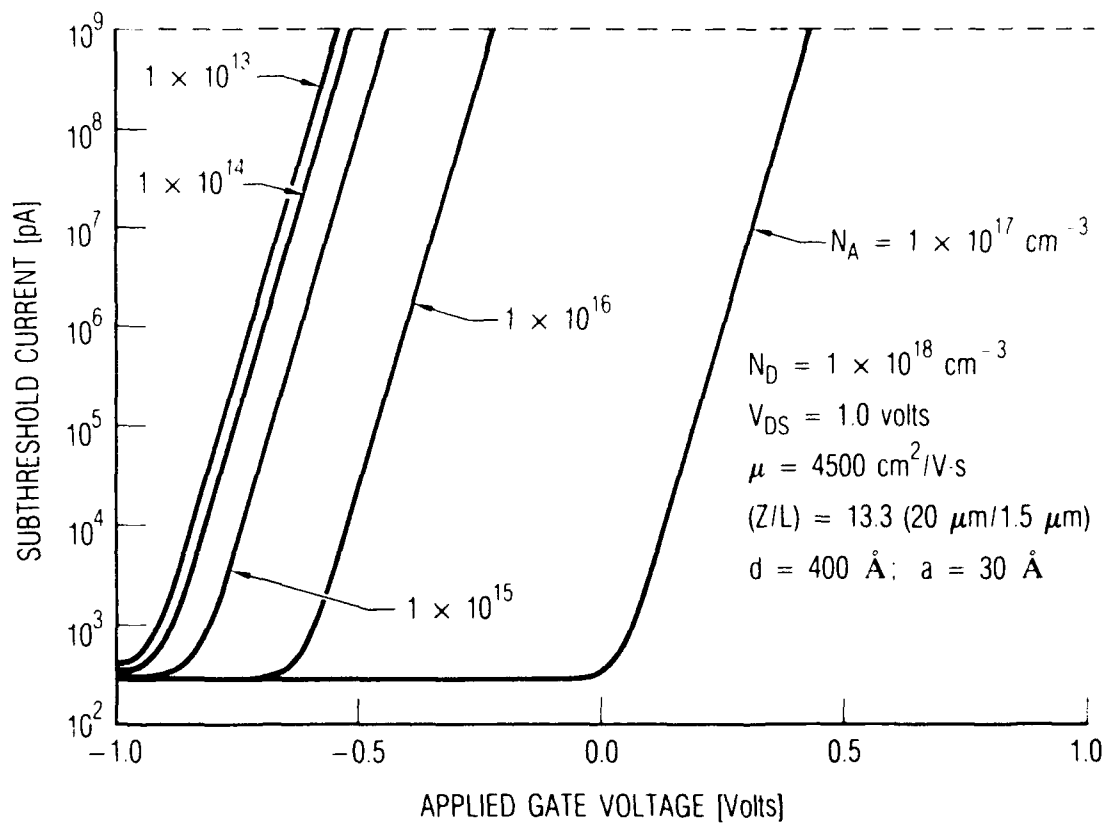


Fig. 3. MODFET Subthreshold Current versus Applied Gate Voltage.

IV. SUMMARY

We have developed a triangular-well, one-subband depletion layer model to describe the dependence of MODFET subthreshold I-V characteristics on AlGaAs and GaAs doping densities and device geometry. The description of the role of acceptor doping on I-V characteristics is important for an accurate description of device performance, especially when MODFETs are used in complementary devices. As has been pointed out previously (Ref. 8), intentional doping of the GaAs may be used to tailor device characteristics for enhanced device performance.

REFERENCES

1. R. J. Krantz and W. L. Bloss, "The Role of Unintentional Acceptor Concentration on the Threshold Voltage of Modulation-Doped Field-Effect Transistors," IEEE Trans. Electron Devices **ED-36**, 451-53 (February 1989).
2. R. J. Krantz, W. L. Bloss, and M. J. O'Loughlin, "High Energy Neutron Effects in GaAs Modulation-Doped Field Effect Transistors (MODFETs): Threshold Voltage," IEEE Trans. Nuc. Sci. **NS-35**, 1438-43 (December 1988).
3. R. J. Krantz and W. L. Bloss, "Threshold Voltage and I-V Characteristics of AlGaAs/GaAs MODFETs," accepted for publication in The Proceedings of the 1989 Industry-University Advanced Materials Conference, Denver, Colorado, March 6-9, 1989.
4. F. F. Fang and W. E. Howard, "Negative Field-Effect Mobility on (100) Si Surfaces," Phys. Rev. Lett. **16**, 797-99 (1966).
5. F. Stern and W. E. Howard, "Properties of Semiconductor Surface Inversion Layers in the Electric Quantum Limit," Phys. Rev. **163**, 816-35 (1967).
6. D. Delagebeaudeuf and N. T. Linh, "Metal-(n) AlGaAs-GaAs Two-Dimensional Electron GaAs FET," IEEE Trans. Electron Devices **ED-29**, 955-60 (June 1982).
7. J. R. Brews, "A Charge Sheet Model of the MOSFET," Solid-State Electron. **21**, 345-55 (1978).
8. M. Shur, "Applications of New Semiconductor Materials for Variable Threshold Field," The Proceeding of the 1989 Industry-University Advanced Materials Conference, Denver, Colorado, March 6-9, 1989.

LABORATORY OPERATIONS

The Aerospace Corporation functions as an "architect-engineer" for national security projects, specializing in advanced military space systems. Providing research support, the corporation's Laboratory Operations conducts experimental and theoretical investigations that focus on the application of scientific and technical advances to such systems. Vital to the success of these investigations is the technical staff's wide-ranging expertise and its ability to stay current with new developments. This expertise is enhanced by a research program aimed at dealing with the many problems associated with rapidly evolving space systems. Contributing their capabilities to the research effort are these individual laboratories:

Aerophysics Laboratory: Launch vehicle and reentry fluid mechanics, heat transfer and flight dynamics; chemical and electric propulsion, propellant chemistry, chemical dynamics, environmental chemistry, trace detection; spacecraft structural mechanics, contamination, thermal and structural control; high temperature thermomechanics, gas kinetics and radiation; cw and pulsed chemical and excimer laser development, including chemical kinetics, spectroscopy, optical resonators, beam control, atmospheric propagation, laser effects and countermeasures.

Chemistry and Physics Laboratory: Atmospheric chemical reactions, atmospheric optics, light scattering, state-specific chemical reactions and radiative signatures of missile plumes, sensor out-of-field-of-view rejection, applied laser spectroscopy, laser chemistry, laser optoelectronics, solar cell physics, battery electrochemistry, space vacuum and radiation effects on materials, lubrication and surface phenomena, thermionic emission, photosensitive materials and detectors, atomic frequency standards, and environmental chemistry.

Electronics Research Laboratory: Microelectronics, solid-state device physics, compound semiconductors, radiation hardening; electro-optics, quantum electronics, solid-state lasers, optical propagation and communications; microwave semiconductor devices, microwave/millimeter wave measurements, diagnostics and radiometry, microwave/millimeter wave thermionic devices; atomic time and frequency standards; antennas, rf systems, electromagnetic propagation phenomena, space communication systems.

Materials Sciences Laboratory: Development of new materials: metals, alloys, ceramics, polymers and their composites, and new forms of carbon; nondestructive evaluation, component failure analysis and reliability; fracture mechanics and stress corrosion; analysis and evaluation of materials at cryogenic and elevated temperatures as well as in space and enemy-induced environments.

Space Sciences Laboratory: Magnetospheric, auroral and cosmic ray physics, wave-particle interactions, magnetospheric plasma waves; atmospheric and ionospheric physics, density and composition of the upper atmosphere, remote sensing using atmospheric radiation; solar physics, infrared astronomy, infrared signature analysis; effects of solar activity, magnetic storms and nuclear explosions on the earth's atmosphere, ionosphere and magnetosphere; effects of electromagnetic and particulate radiations on space systems; space instrumentation.